Respiratory Research

RESEARCH

Open Access

Dysregulated metabolic pathways of pulmonary fibrosis and the lipids associated with the effects of nintedanib therapy

Yasuo Shimizu[1*], Yasuhiro Horibata[2], Mariko Domae[2], Yusuke Nakamura[1], Tatsuya Yokoyama[1], Ryo Arai[1], Taichi Shiobara[1], Akihiro Takemasa[1], Ryosuke Koike[1], Nobuhiko Uchida[1], Meitetsu Masawa[1], Rinna Tei[1], Taiji Watanabe[1], Hiroko Morita[1], Masaaki Miyoshi[1], Sayo Soda[1], Seiji Niho[1], Ko Igami[3] and Hiroyuki Sugimoto[2]

Abstract

Background Pulmonary fibrosis (PF) is a disease with a poor prognosis, and its pathogenesis is not fully understood. Identifying dysregulation of lipid metabolism in PF may provide insight and promote the development of novel therapies. The present study was designed to clarify the dysregulated lipid pathways and identify lipids correlated with treatment response.

Methods This research comprised two prospective cohort studies. Study 1 aimed to identify dysregulated metabolic pathways and lipids in the peripheral blood of PF patients, compared with healthy control (HC) subjects. Study 2 aimed to identify lipids associated with the decline in % forced vital capacity (%FVC) and survival in PF patients treated with the anti-fibrotic drug, nintedanib. As a preliminary ancillary experiment, we attempted to identify the lipids associated with endothelial cells and fibroblasts.

Results In Study 1, 38 lipids were identified that differed between the PF ($n=66$) and HC ($n=63$) groups. Compared with the HC subjects, phosphatidylcholine (PC) 36:5 was the most up-regulated and lysophosphatidylcholine (LPC) 18:0 was the most down-regulated in PF patients. Glycerophospholipid metabolism was the most enriched pathway. Plasmenyl phosphatidylethanolamine (pPE) and plasmanyl phosphatidylcholine (pPC) were determined to be endothelial-related lipids, and phosphatidylethanolamine (PE) were fibroblast-related lipids in PF. In Study 2, 10 lipids were identified that differed between the absolute decline in %FVC < 2.5% group (6 M responders, $n=14$) and the decline in %FVC > 2.5% group (6 M non-responders, $n=6$) after 6 M of nintedanib therapy, and 6 lipids were identified that differed between the absolute decline in %FVC < 5% group (12 M responders, $n=15$) and the decline in %FVC > 5% group (12 M non-responders, $n=5$) after 12 M of nintedanib therapy. Four lipids were consistently detected at 6 M and 12 M, and among them, higher levels of pPE 18:0p/22:6 at 6 M showed a poorer prognosis for 24 M survival ($p<0.05$, HR = 6.547, 95% CI = 1.471–29.13). Under nintedanib therapy, pPE species were correlated with progressive fibrosis, and pPE 18:0p/22:6 was considered an endothelial-related lipid.

*Correspondence:
Yasuo Shimizu
yasuo-s@dokkyomed.ac.jp

Full list of author information is available at the end of the article

Conclusions Lipidomic profiling revealed distinct pathways in PF patients. pPE species were strongly associated with the responses to nintedanib therapy. Targeting the lipids or catabolic enzymes involved in dysregulated pathways has the potential to ameliorate PF.

Trial registration Registry for UMIN, Lipidomic analysis on plasma in idiopathic pulmonary fibrosis patients. Trial registry number, UMIN000020872. Registered 3 February 2016, https://center6.umin.ac.jp/cgiopenbin/ctr/index.cgi.

Keywords Metabolic dysregulation, Lipidomics, Endothelial cells, Myofibroblasts, Pulmonary fibrosis, Vasculature, LC-MS, Nintedanib, Plasmalogen, Plasmenyl phosphatidylethanolamine

Introduction

Idiopathic pulmonary fibrosis (IPF) is characterized by the progressive worsening of dyspnea and lung function and is associated with a poor prognosis [1]. Metabolic alterations are increasingly being recognized as important pathogenic processes that underlie fibrosis across various organs [2]. Strategies that target metabolic dysregulation in fibrosis may be effective in treating pulmonary fibrosis (PF), and such treatments are eagerly awaited.

Lipids are often considered for evaluating the condition of cells and tissues, and thus, to realize personalized medicine for PF, it is necessary to examine the lipids associated with the disease pathways of PF and the changes of different cell types or response of cells to anti-fibrotic drugs such as nintedanib.

The pathogenesis of PF involves functional abnormalities in cells and morphological changes of airway epithelial cells and fibroblasts, as well as vascular endothelial cell injury [3, 4]. Transformations with morphological changes, such as fibroblasts to myofibroblasts, are also accompanied by changes in intracellular lipid metabolism-associated genes and protein expression [5, 6]. Furthermore, increased endothelial cell activation and phenotypically abnormality drive PF, which suggests that PF is related to vascular disease [7].

Nintedanib is an inhibitor of the vascular endothelial growth factor receptor (VEGF-R), platelet-derived growth factor receptor (PDGF-R), and fibroblast growth factor receptor (FGF-R) [8]. VEGF, PDGF, and FGF play important roles in the development of fibrovascular lesions in PF [9]. Accordingly, nintedanib can affect endothelial cells and fibroblasts in the lungs of PF patients, and identifying the lipids that correlate with the effects of nintedanib on these cells may be useful in determining the optimal time course of nintedanib treatment and the PF patients who are expected to respond most effectively.

Previous studies demonstrated that cellular phospholipids levels change during the differentiation and maturation of human induced pluripotent stem cells (iPSCs) into vascular endothelial cells [10]. Lysophosphatidylcholines (LPCs) were involved in the two-dimensional network formation of vascular endothelial cells used as a model for the repair and regeneration processes of endothelial cell networks [11]. Phospholipid levels changed during the transformation from human fibroblasts to myofibroblasts stimulated by TGF-β, reflecting a defect in lipid synthase in the intracellular mitochondria [12].

The primary purpose of the present study was to identify lipids and metabolic pathways in the peripheral blood of PF patients and determine the differences in lipid metabolic behaviors between the PF patients and healthy control (HC) subjects (Study 1). The second purpose was to identify lipids associated with decreased lung function at 6 M and 12 M in PF patients treated with the anti-fibrotic drug, nintedanib, and we examined whether these lipids were associated with the prognosis of PF patients (Study 2).

As an ancillary analysis, we compared the lipids detected in the patients' plasma with the results obtained from our lipid analyses at the cellular level. That is, we aimed to determine the lipids reflecting fibroblast-to-myofibroblast transformation (fibroblast-related lipids) or matured endothelial cells (endothelial-related lipids), referencing previous in vitro studies [10–12].

Patients and methods

Subjects

IPF patients who visited the Department of Pulmonary Medicine and Clinical Immunology, Dokkyo Medical University Hospital between February 2016 and March 2021 and agreed to participate in this study were enrolled. The diagnosis of IPF was made by the physicians based on the official guidelines reported by the American Thoracic Society/European Respiratory Society/Japanese Respiratory Society/Latin American Thoracic Association (ATS/ERS/JRS/LATA) [1]. A surgical lung biopsy was not necessarily required for diagnosis. The following exclusion criteria were established: patients under 16 years of age, patients with lung cancer or previous surgery for lung cancer or other pulmonary diseases, patients with combined pulmonary fibrosis and emphysema, and patients who did not consent to this study.

Study design

The main research comprised two studies, namely Study 1 and Study 2 (Fig. 1). Study 1 was designed to identify

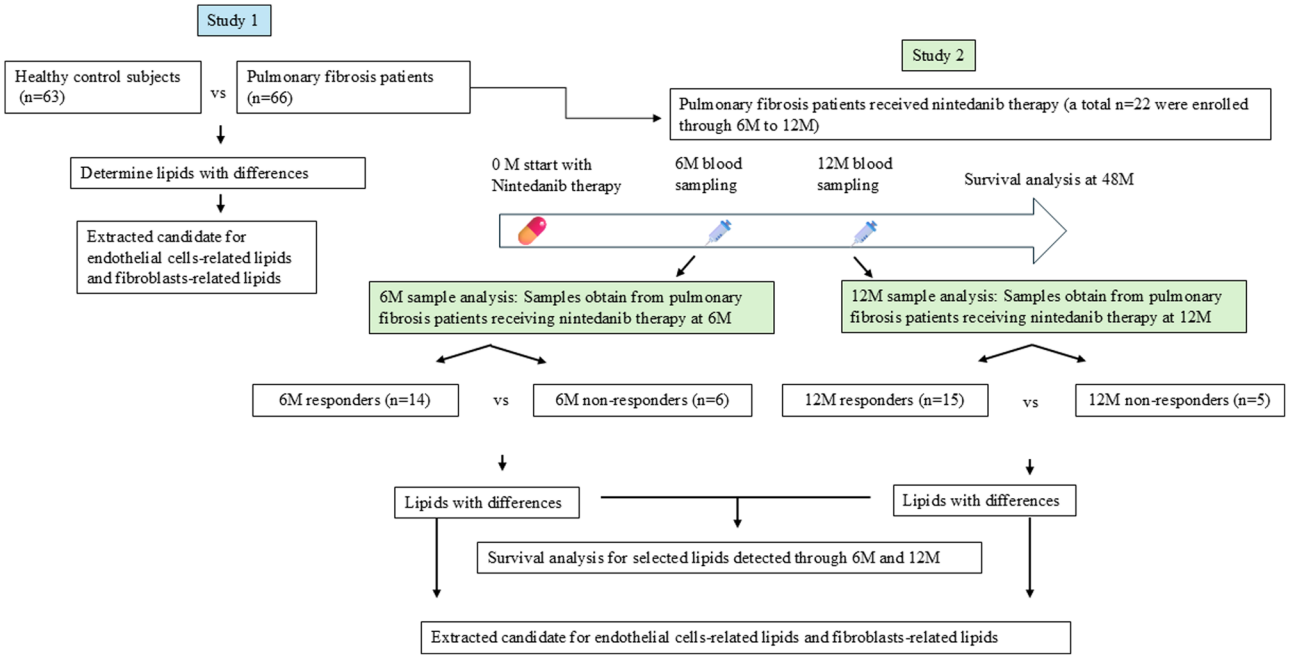

Fig. 1 Diagram illustrating the outline of the present research, consisting of Study 1 and Study 2. Study 1 was designed to identify unique lipid species and metabolic pathways in the peripheral blood of PF patients compared with HC subjects. Study 2 was designed to identify lipids related to the degree of absolute decline in %FVC at 6 M and 12 M after starting nintedanib. The PF patients enrolled in Study 2 were those enrolled in Study 1 who agreed to take anti-fibrotic medication. Patients were divided with an absolute decline in %FVC < 2.5% (less decline, 6 M responders) and those with a decrease in %FVC ≧ 2.5% (more decline, 6 M non-responders) 6 M after starting nintedanib, and absolute decline in %FVC < 5% (less decline, 12 M responders) and those with a decrease in %FVC ≧ 5% (more decline,12 M non-responders) 12 M after starting nintedanib. As an ancillary experiment, we investigated whether the lipids extracted in Study 1 and Study 2 contained candidates specifically related to endothelial cells or fibroblasts

lipid species and metabolic pathways in the peripheral blood of IPF (simply referred to as PF hereafter) patients, who were expected to exhibit different lipid metabolic behaviors compared with HC subjects. Lipids in the peripheral blood of HC ($n = 63$) and PF ($n = 66$) patients were compared. To match the background of the PF patients, plasma was obtained from elderly Asians to represent the HC subjects (Tokyo Future Style, Inc, Tsukuba, Ibaraki, Japan). Plasma was collected from PF patients who were not taking prednisolone or anti-fibrotic drugs, such as nintedanib or pirfenidone, at the entry of Study 1 (Fig. 1). Peripheral blood samples were taken from 8:30 AM to11:00 AM in a fasting state and stored at − 80℃ until analysis.

Study 2 was designed to identify lipids related to the decrease in absolute changes of %FVC at 6 M and 12 M after starting nintedanib administration. The majority (18/20) of the PF patients enrolled in Study 2 were those enrolled in Study 1 who agreed to take nintedanib. To determine the lipids that reflect the effect of nintedanib against lung function decline, we compared lipids in blood samples taken from patients with an absolute decline in %FVC < 2.5% (less decline, 6 M responders) and those with a decrease in %FVC ≧ 2.5% (more decline, 6 M non-responders) 6 M after starting nintedanib. Next, we compared lipids in blood samples taken from patients with an absolute decline in %FVC < 5% (less decline, 12 M responders) and those with a decrease in %FVC ≧ 5% (more decline,12 M non-responders) 12 M after starting nintedanib. Furthermore, to investigate the relationship between lipids levels and 24 M survival, patients were divided into two groups, namely those with lipid levels above or below the mean.

As an ancillary experiment, we determined the lipids reflecting endothelial cells and fibroblasts by referencing previous in vitro studies performed in our laboratory (Table S1) [10–12]. Endothelial cell-related lipids were determined from the extracted lipids that increased during endothelial cell development, exhibited higher levels in endothelial cells than fibroblasts, or were abundant during endothelial network formation [10, 11, 13]. Fibroblast-related lipids were identified as lipids showing a change in levels during the transition from fibroblasts to myofibroblasts [12].

Pulmonary function tests

Pulmonary function tests (FUDAC-7 or FUDAC-77, Fukuda Denshi, Tokyo, Japan) were performed at the time of blood sampling. Patients enrolled only in Study 1 had their blood drawn and lung function tested only once, whereas patients enrolled in both Study 1 and Study 2 had their blood drawn and lung function tested

in the first study and again 6 M and 12 M after the initiation of nintedanib therapy. An allowance of 2 M before and after the defined date was provided for measurement and data acquisition.

Extraction and quantification of lipids by liquid chromatography-tandem mass spectrometry (LC-MS/MS)

Total lipids were extracted from plasma (50 µl) using 1 ml of methanol containing 0.5–1 nmol of the internal standard (Table S2). After vortexing and centrifugation at 25,000 g for 10 min, lipids were collected and stored at − 80℃ after sealing under nitrogen. The content of each lipid species was quantified by reverse-phase high-pressure liquid chromatography, as previously described with minor modification, using a 5500 QTRAP mass spectrometer (Sciex Inc., Framingham, MA) equipped with an L-column 2 ODS column (3 µm, 2.0 mm × 100 mm) (Chemicals Evaluation and Research Institute, Tokyo, Japan) [10]. A binary gradient consisting of solvent A (acetonitrile: methanol: water, 1:1:3, v/v/v, containing 5 mM ammonium acetate and 1% formic acid) and solvent B (2-propanol containing 5 mM ammonium acetate and 1% formic acid) was used. The following gradient profile was employed: 0–1 min, 95% A; 1–3 min, 5–95% B linear gradient; 3–5 min, 95% B. The flow rate was 0.2 ml/min, and the column temperature was maintained at 40℃. Lipids were quantified using MultiQuant version 3.0 (Sciex Inc) and normalized against the internal standard.

Statistical analysis and data integration

The age and physiology index were indicated using the mean and interquartile range, and the body surface area was calculated using the Du Bois method. For PF patients and HC subjects, age was compared using nonparametric tests, followed by the Mann–Whitney test, and gender was compared using Fisher's exact test. Metaboanalyst 6.0 was used in the analysis of lipid values obtained by LC-MS/MS [14]. Differences between the two groups were filtered based on the log fold change (FC) (either > or < 1.5) and the false discovery rate (FDR) with $p < 0.05$. Metaboanalyst 6.0 was also used to determine the enriched metabolic pathways by inputting the FC obtained for lipids according to the comparison between groups. Kyoto Encyclopedia of Genes and Genomes (KEGG) IDs were assigned to lipids for pathway analysis. Pathview was used to chart the metabolic pathways of glycerophospholipid, sphingolipid, and ether lipid metabolism [15, 16]. Spearman's correlation coefficient by rank was used to examine correlation between the lipid and the baseline %FVC with the 95% confidence interval (CI) and Kaplan–Meier analysis was employed to compare survival between groups, and the hazard ratio (HR) was calculated with the 95% CI using GraphPad Prism 10.3.1. A p-value < 0.05 was considered significant.

Table 1 Characteristics and baseline demographics of healthy volunteers and pulmonary fibrosis patients in study 1

Parameters	Healthy volunteers (*n*=63)	Pulmonry fibrosis (*n*=66)	*P* value
Age, years	65, (58-72)	72, (67-77)	$p<0.05$
Gender, Male/Female	38/25	55/11	$p<0.05$
Smoking history, pack-years		20 (3.0-40.0)	
Current, former, never, (%)		3, 75.8, 21.2	
BMI		23.0, (19.5-25.5)	
BSA (m2)		1.65 (1.50-1.74)	
FEV1/FVC (G)(%)		85.8 (80.2-91.7)	
FVC (ml)		2070 (1705-2535)	
%FVC (%)		67.2 (57.6-81.1)	
mMRC		2 (0-3)	
KL-6 (U/mL)		1120 (660.0-1775)	
Comorbidities, n (%)			
Hypertension		17 (25.8)	
Diabetes Mellitus		16 (24.2)	
Hyper lipidemia		9 (13.6)	
Benign prostatic hyperplasia		7 (10.6)	
Hyperuricemia		5 (7.6)	
Chronic kidney disease		4 (6.1)	

Data were expressed as mean and interquartile range (IQR)

Table 2 **A** characteristics of patients included in the analysis 6 months after initiation of nintedanib treatment in study 2

Parameters	6 M responders (*n*=14)	6 M non-responders (*n*=6)	*P* value
Age, years	74.5 (67-78)	71.5 (68.3-75)	n.s
Gender, Male/Female	10/4	4/2	n.s
BMI	23.6 (18.9-26.4)	23.5 (20.3-27.4)	n.s
BSA (m2)	1.61 (1.53-1.70)	1.74 (1.54-1.90)	n.s
FEV1/FVC (G)(%)	87.1 (80.8-91.3)	87.1 (80.4-87.1)	n.s
FVC (ml)	2170 (1758-2463)	1980 (1195-2503)	n.s
%FVC (%)	68.9 (52.9-76.0)	61.3 37.1-81.1)	n.s
KL-6 (U/mL)	943.5 (538.8-1800)	1140 (754.0-1788)	n.s

Data were expressed as mean and interquartile range (IQR)

Results

Clinical characteristics of the patients in study 1

In Study 1, the PF group was older and more male than the HC group ($p < 0.05$). None of the patients who were enrolled underwent a surgical biopsy for the diagnosis of PF. The low %FVC of 66.9% and high KL-6 of 1020 U/ml in the PF group suggested that the enrolled population had restrictive pulmonary dysfunction, presenting active PF (Table 1).

Pulmonary fibrosis patients have unique lipid metabolism

Principal component analysis (PCA) was employed for PC1 and PC2, showing the separate distributions in the

HC and PF groups (Fig. 2A). A heatmap illustrates the different expression patterns between the two groups (Fig. 2B). Different lipids were confirmed for the different expression patterns and extracted using the log FC differences of the PF to HC values (PF/HC) and FDR with $p < 0.05$, and a total of 41 lipids were extracted, as shown in the volcano plot. Phosphatidylcholine (PC) 36:5 was the most up-regulated, and LPC 18:0 was the most down-regulated in the PF group. (Fig. 2C). Three lipids showing up-regulation in PF patients (i.e., dihydrosphingosine 1-phosphate d18:0 (S1P d18:0), ceramide d18:1/20:0 (Cer d18:1/20:0), and plasmenyl ethanolamine (pPE) 18:1p/18:1) were excluded because these lipids had outlier values, as confirmed in the box-and-whisker plots (Fig. S1). Thus, a total of 38 lipids were identified that differed between the PF and HC groups. Among 38 lipids, 9 lipids were up-regulated and 29 were down-regulated in PF (Fig. 2D). A heatmap was also generated for the 38 lipids, categorized between the PF and HC groups (Fig. 2E).

An orthogonal partial least square-discriminant analysis (OPLS-DA) was performed on all lipids to create a model that discriminates between the PF and HC groups. A good discrimination model was obtained with R2Y = 0.764, indicating more than 0.65 R2Y, and Q2Y = 0.745, indicating more than 0.5 Q2Y (Fig. 3A). Next, to identify the lipids that enable strong discrimination between PF and HC patients, a variable importance for projection (VIP) analysis was performed based on the results of the OPLS-DA analysis, and 47 lipids were identified with VIP scores > 1.0. LPC 18:0 exhibited the highest VIP score (Fig. 3B).

Next, we attempted to narrow down the lipids having both high discriminatory ability and significant differences in expression between the PF and HC groups (Fig. 3C). Among the lipid candidates selected based on the logFC values and VIP scores, the lipids showing the top three VIP scores with valuable logFC values were LPC 18:0, lysophosphatidic acid (LPA) 18:2, and LPA 20:4, which were down-regulated in PF. PC 36:5, plasmanyl phosphatidylcholine 38p:0 (pPC 38p:0), and phosphatidylethanolamine (PE) 38:6 were up-regulated in PF, and these lipids had medium to low VIP scores (Fig. 3C and D). There were no correlations between these lipids (i.e., LPC 18:0, LPA 18:2, LPA 20:4, PC36:5, pPC 38p:0, PE 38:6) and the baseline %FVC (data not shown).

Dysregulation of lipid metabolic pathways underlying PF pathophysiology

The lipids with valuable logFC values shown in Fig. 2D and E (after exclusion of three lipids) were subjected to pathway analysis. Glycerophospholipid, sphingolipid, and ether lipid metabolism were enriched in PF (Fig. 4A). Glycerophospholipid metabolism was the most enriched pathway, including LPC 18:0 (down-regulated in PF) and PC 36:5 (up-regulated in PF). LPC was down-regulated in PF, suggesting the dysregulation of lecithin-cholesterol acyltransferase (LCAT) and phospholipase A2 (PLA2), which are enzymes involved in the conversion of PC to LPC, or the dysregulation of lysophosphatidylcholine acyltransferase (LPCAT), which is an enzyme involved in the conversion of LPC to PC. Lysophosphatidylethanolamine (LPE) was also down-regulated in PF, suggesting the dysregulation of PLA2, which is involved in the conversion of PE to LPE, or the dysregulation of lysophosphatidylethanolamine acyltransferase (LPEAT), which is an enzyme involved in the conversion of LPE to PE. Furthermore, LPA was down-regulated in PF, which was attributed to down-regulated LPC and LPE or dysregulated autotaxin (ATX) (Fig. 4B and C, and S2).

Sphingolipid metabolism was the next most enriched pathway, including S1P d18:1 (down-regulated in PF). Cer d18:0/24:0 was catabolized to Cer 18:1/16:0 by sphingolipid delta 4-desaturase in the ceramide biosynthesis pathway, and both ceramides were down-regulated in PF (Figs. S3 and S4). Ether lipid metabolism was the third most enriched pathway, involving 7 lipids, including pPC 38p:0 and pPE 18:0p/20:5 (up-regulated in PF); however, it did not exhibit a promising pathway directly connecting the fluctuating pPC and pPE (Figs. S5 and S6).

Some lipids May reflect changes in endothelial cells and fibroblasts in PF

The 38 lipids extracted based on their logFC values were referenced as endothelial-related or fibroblast-related lipids (Table S1). Compared with the HC group, up-regulated pPE 38p:5 was a candidate for endothelial-related lipids, and up-regulated PE 32:1 and down-regulated PE 40:4 were candidates for fibroblast-related lipids in PF (Fig. S7).

Clinical characteristics of the patients in study 2

In Study 2, lipids related to the absolute decline in %FVC 6 M and 12 M after starting nintedanib therapy were identified. At 6 M, there were no significant differences in patient background between the 6 M responders ($n = 14$) and 6 M non-responders ($n = 6$) (Table 2A). One patient enrolled in the 6 M non-responders died at 4 M, but that patient was considered in the 6 M group because the allowance for the data acquisition was ± 2 M. At 12 M, there were also no differences in the patient background between the 12 M responders ($n = 15$) and 12 M non-responders ($n = 5$) (Table 2B). Although the patients involved in the 6 M analysis were not completely the same patients as those involved in the 12 M analysis, 90% (18/20) of the patients enrolled in the 12 M analysis had been enrolled in the 6 M analysis.

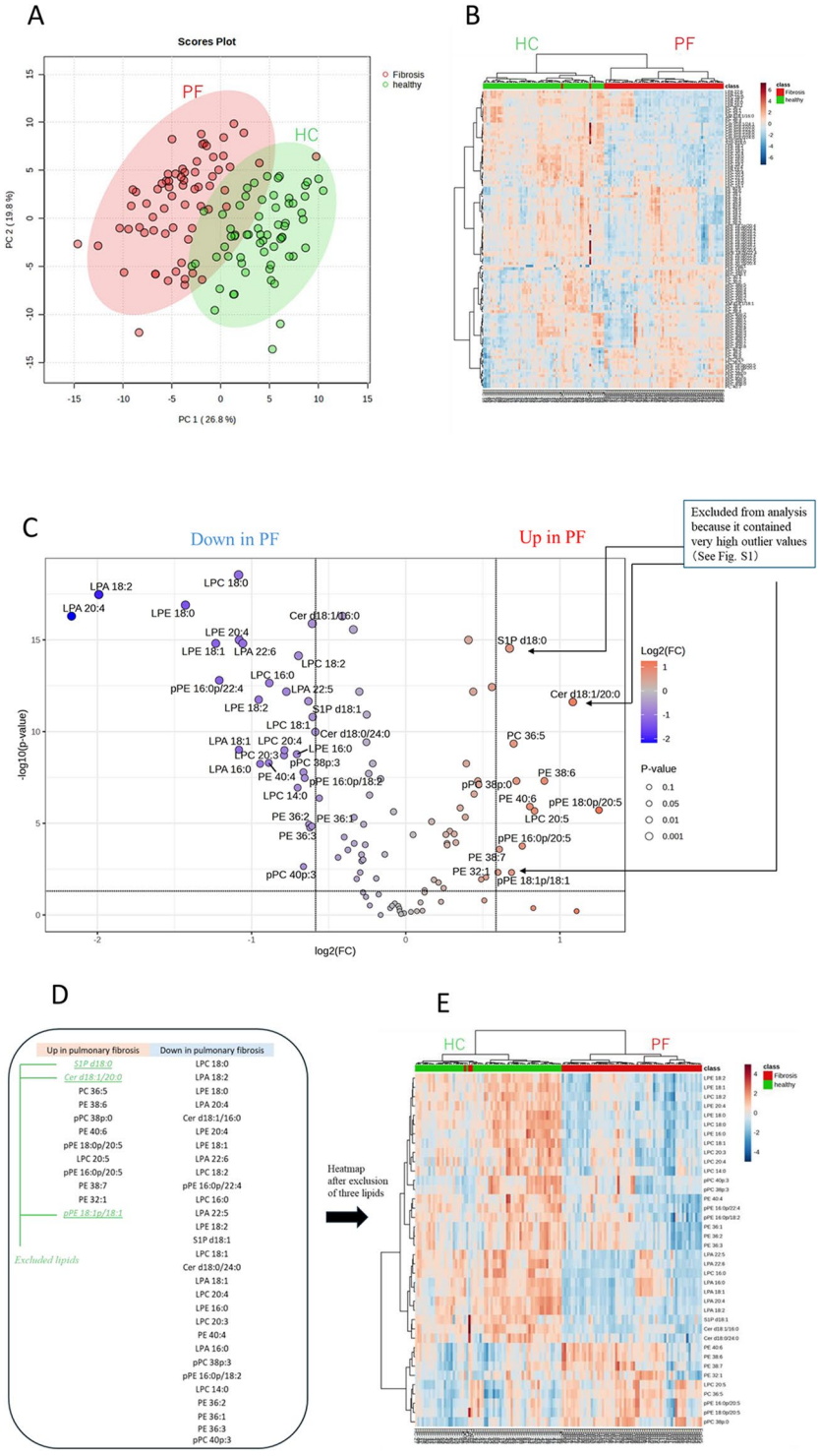

Fig. 2 PCA and heatmaps of the lipids examined in the present study. (**A**) PCA analysis of the lipids from PF patients and HC subjects. (**B**) Heatmap of the lipids. Each column in the heatmap showed blue for down-regulation and red for up-regulation. PF patients (red) and HC subjects (green) were indicated as groups. (**C**) Volcano plot depicting differential expression of all lipids between PF patients and HC subjects. Lipids that increased in PF patients are indicated in red, and those that decreased are indicated in purple (a total of 41 lipids). (**D**) A list of all 41 lipids, including the three lipids with outlier values. Three lipids contained outlier values (indicated in green italics), as confirmed in the box-and-whisker plots (Fig. S1). Those lipids were excluded from the subsequent heatmap analysis. (**E**) Heatmap of the lipids from PF patients and HC subjects after excluding the three lipids with outlier values (a total of 38 lipids)

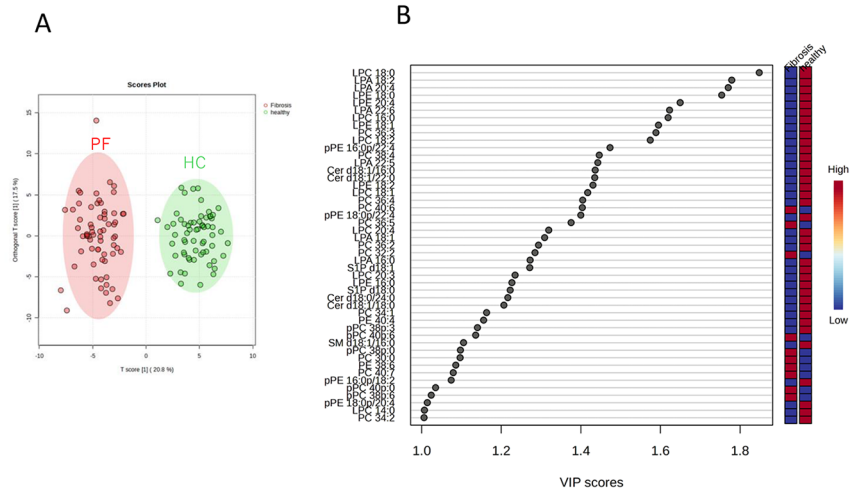

C

Lipids in VIP score	VIP score	LogFC (Volcano plot)
LPC 18:0	1	down
LPA 18:2	2	down
LPA 20:4	3	down
LPE 18:0	4	down
LPE 20:4	5	down
LPA 22:6	6	down
LPC 16:0	7	down
LPE 18:1	8	down
PC 36:3	9	n/d
LPC 18:2	10	down
pPE 16:0p/22:4	11	down
PC 38:4	12	n/d
LPA 22:5	13	down
Cer d18:1/16:0	14	down
Cer d18:1/22:0	15	n/d
LPE 18:2	16	down in PF
LPC 18:1	17	down in PF
PC 36:4	18	n/d
PC 40:6	19	n/d
pPE 18:0p/22:4	20	n/d
PC 36:5	21	up
LPC 20:4	22	down
LPA 18:1	23	down
PC 36:2	24	n/d
PC 32:2	25	n/d
LPA 16:0	26	down
S1P d18:1	27	down
LPC 20:3	28	down
LPE 16:0	29	down
SIP d18:0	30	n/a
Cer d18:1/24:0	31	down
Cer d18:1/18:0	32	n/d
PC 34:1	33	n/d
PE 40:4	34	down
pPC 38p:3	35	down
pPC 40p:6	36	n/d
SM d18:1/16:0	37	n/d
pPC 38p:0	38	up
PC 30.0	39	
PE 38:6	40	up
PC 40:7	41	n/d
pPE 16:0p/18:2	42	down
pPC 40p:0	43	n/d
pPC 38p:6	44	n/d
pPE 18:0p/20:4	45	n/d
LPC 14:0	46	down
PC 34:2	47	n/d

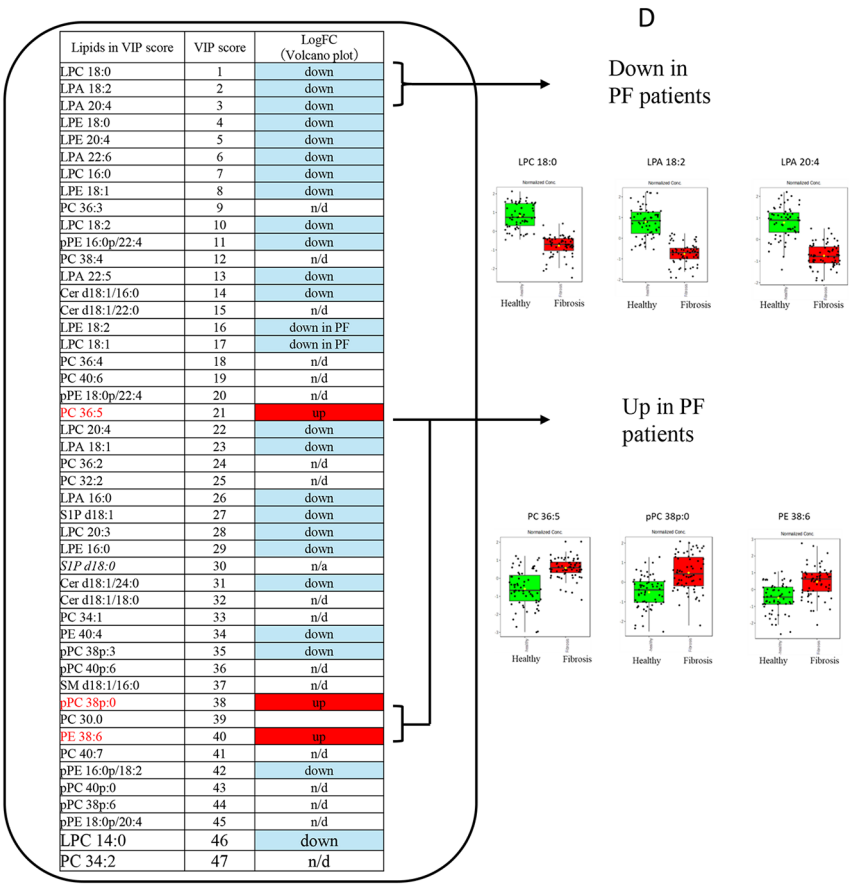

Fig. 3 (**A**) The OPLS-DA of PF patients and HC subjects. (**B**) VIP scores for extracted lipids that help discriminate between PF patients and HC subjects. The vertical axis indicates the lipids, and the horizontal axis indicates the VIP scores. (**C**) List of lipids with both a valuable VIP score and logFC value. n/d: not detected. (**D**) Distribution of each lipid in the top 3 ranked lipid species indicated using box-and-whisker plots. The top 3 ranked lipids by VIP score were down-regulated in PF, whereas the up-regulated lipids exhibited medium to low VIP scores

Lipid levels associated with the suppressive effects of nintedanib on pulmonary function decline

In the comparison of lipids between the responders and non-responders, PCA could not be leveraged to distinguish between the groups, like in Study 1, because the subjects were all PF patients, but the two groups could be separated based on the OPLS-DA. Considering the VIP scores, PC 38:4 was the top-scoring lipid

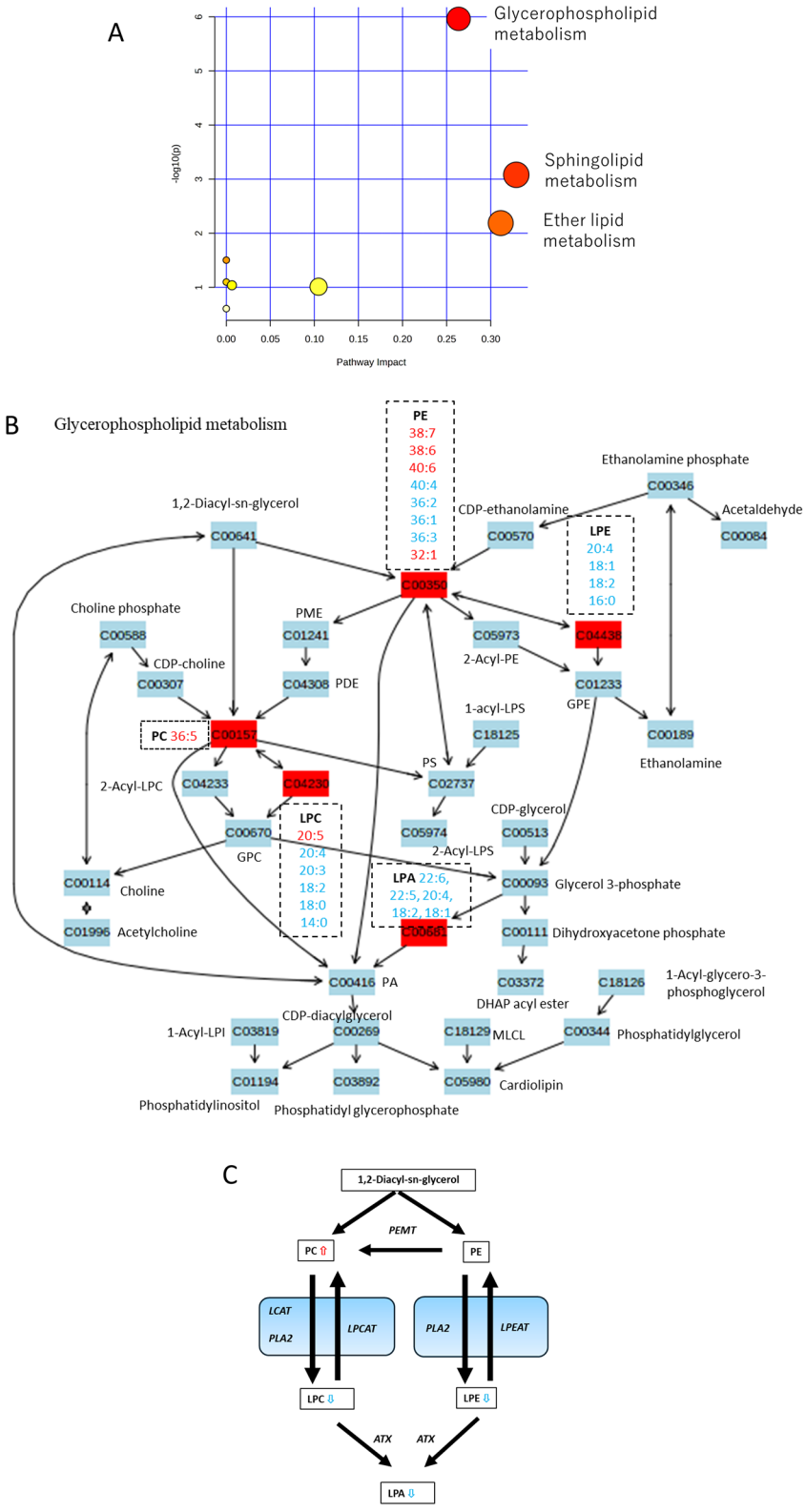

Fig. 4 (See legend on next page.)

(See figure on previous page.)

Fig. 4 (**A**) Enriched lipid pathways in the comparison between PF patients and HC subjects in Study 1. (**B**) Enriched pathway of glycerophospholipid metabolism. Pathways were generated using Metaboanalyst. Each number in the box denotes the KEGG ID of the lipid. Red boxes indicate lipids detected in the present study, and those lipids were listed in the dotted-line boxes. Red lipids indicate up-regulation in PF, whereas blue lipids indicate down-regulation in PF. (**C**) Metabolic pathways of LPC and LPE. 1,2-diacyl-sn-glycerol is converted to PC and PE. PC can be delivered from PE by phosphatidylethanolamine/phosphatidyl-N-methylethanolamine N-methyltransferase (PEMT). PC is catabolized to LPC by lecithin-cholesterol acyltransferase (LCAT) and phospholipase A2 (PLA2), and lysophosphatidylcholine acyltransferase (LPCAT) synthesizes PC from LPC. PE is catabolized to LPE by PLA2, and lysophosphatidylethanolamine acyltransferase (LPEAT) synthesizes PE from LPE. LPC and LPE are converted to LPA by autotaxin (ATX)

for discriminating between the 6 M responders and 6 M non-responders at 6 M, and PC 38:4 was up-regulated in the 6 M responders, meaning it was down-regulated in the 6 M non-responders. pPE 18:0p/22:6 was the top-scoring ether lipid for discriminating between the 12 M responders and 12 M non-responders at 12 M. pPE 18:0p/22:6 was down-regulated in the 12 M responders and up-regulated in the12M non-responders (Fig. S8).

There were 10 lipids that showed differences in the logFC values between the 6 M responders and 6 M non-responders at 6 M. LPA 16:0, pPC, and pPE were down-regulated in the 6 M responders, indicating that these lipids were up-regulated in patients showing a decline of more than 2.5% in %FVC, despite 6 M of nintedanib therapy (Fig. 5A). There were 6 lipids that showed differences in the logFC values between the 12 M responders and 12 M non-responders at 12 M, and pPE lipids were down-regulated in the 12 M responders, indicating that these lipids were up-regulated in the 12 M non-responders despite 12 M of nintedanib therapy (Fig. 5B). There were 4 extracted lipids at both 6 M and 12 M (Fig. 5C). From 6 M to 12 M, LPE 14:0 was up-regulated in patients with less lung function decline (i.e., down-regulated in the 6 M non-responders and 12 M non-responders), whereas pPE 16:0p/22:6, pPE 18:0p/22:6, and pPE 18:0p/18:2 were down-regulated in patients with less lung function decline (i.e., up-regulated in the 6 M non-responders and 12 M non-responders), as confirmed in the box-and-whisker plots (Fig. 5C and D). There were no correlations between the lipids (i.e., LPE 14:0, pPE 18:0p/18:2, pPE 18:0p/22:6, pPE 16:0p/22:6) at 6 M or 12 M and the %FVC in each month (data not shown).

Patients with elevated levels of Plasmenyl PE had a poor prognosis despite nintedanib treatment

Patients were divided into two groups based on the median level of each pPE lipid at 6 M (i.e., the above median and below median groups), and the two groups were compared regarding the survival at 24 M after starting nintedanib therapy. Patients with levels above the median for pPE 18:0p/22:6 at 6 M had a poorer prognosis than those with levels below the median ($p < 0.05$, HR = 6.547, 95% CI = 1.471–29.13) (Fig. 5E). The other 3 lipids did not show significant differences. In the same way, these 4 lipids were examined at 12 M for 24 M survival, but no significant differences were found (data not shown).

Some lipids related to differences in the response to nintedanib treatment May mirror the dysregulation of endothelial cells and fibroblasts in PF

The investigation of endothelial cell- and fibroblast-related lipids in Study 2 revealed that pPE 18:0p/18:2 and pPE 18:0p/22:6 were endothelial-related and down-regulated in the 6 M responders and 12 M responders (i.e., up-regulated in the 6 M non-responders and 12 M non-responders), indicating greater lung function decline. Patients with a pPE 18:0p/22:6 level higher than the median at 6 M had a worse prognosis than those with a pPE 18:0p/22:6 level lower than the median (the data are also shown in Fig. 5E), but there was no significant difference for pPE 16:0p/22:6 at 12 M (Fig. 6A and B). At 12 M, both pPE 18:0p/22:6 and pPE 16:0p/22:6 did not show significant differences in prognosis (data not shown).

The investigation also revealed that pPE 18:0p/18:2, pPE 16:0p/18:1, and PC 38:4 were fibroblast-related lipids. Myofibroblasts contribute to PF and the progression of lung function decline; therefore, it is assumed that lipids that are down-regulated in responders/non-responders (up-regulated in myofibroblasts) or up-regulated in responders/non-responders (down-regulated in myofibroblasts) were regarded as PF aggravation lipids. A comparison of the survival between the lipids with levels above and below the median at 6 M did not show a significant relationship with 24 M survival, for each of these 3 lipids. pPE 18:0p/18:2 could be detected at both 6 M and 12 M, but the levels at 12 M did not show a significant relationship with 24 M survival (data not shown).

Discussion

Circulating lipid levels were found to significantly differ between PF patients and HC subjects. The glycerophospholipid metabolism, sphingolipid metabolism, and ether lipid metabolism pathways were altered in PF.

Glycerophospholipid metabolism and lipid levels were dysregulated in PF

Among the lipids involved in glycerophospholipid metabolism, pathways responsible for the synthesis and degradation of LPC, LPE, and LPA were suggested to be dysregulated, and the levels of these lipids were lower in the PF group than in the HC group. As mechanisms for the decrease in LPC, the loss of alveolar type 2 cells may be the source of LPC and the activation of ATX, which catabolizes LPC to LPA [17, 18]. Conversely, an

Table 2 **B** characteristics of patients included in the analysis 12 months after initiation of nintedanib treatment in study 2

Parameters	12 M responders (*n*=15)	12 M non-responders (*n*=5)	*P* value
Age, years	74.0 (70-79)	71 (62-76)	n.s
Gender, Male/Female	11/4	3/2	n.s
BMI	23.3 (20.0-25.4)	23.4 (18.5-31.2)	n.s
BSA (m2)	1.62 (1.57-1.68)	1.81 (1.44-1.93)	n.s
FEV1/FVC (G)(%)	86.9 (83.8-93.8)	89.0 (83.0-90.5)	n.s
FVC (ml)	2180 1890-2600)	2190 (980-2210)	n.s
%FVC (%)	71.1 (56.7-76.4)	54.2 (34.2-75.2)	n.s
KL-6 (U/mL)	1136 (499-1620)	1020 649-1580)	n.s

Data were expressed as mean and interquartile range (IQR)

increase in LPC has been reported in PF by activation of PLA2G2A, which catabolizes PC to LPC [19, 20]. Considering that lysophosphatidylcholine acyltransferase (LPCAT) converts LPC to PC, the balance of catabolic enzymes for synthesis and degradation may be involved in PF pathogenesis.

LPC 18:0 showed the highest VIP score and was considered useful for discriminating PF patients from HC subjects. LPC was reported to play inflammatory, anti-hemostatic, and cytotoxic roles, while exhibiting anti-inflammatory effects [21]. The decrease in LPC in PF has also been reported in previous reports, consistent with the present study [17]. Decreased LPC 18:0 was associated with a decline in %FVC > 10%, decline in DLCO > 15%, or death within 2 years, indicating that LPC18:0 was reduced in severe advanced IPF [17]. It has also been reported that LPC 18:0 and LPC 14:0 were reduced in the acute phase of drug-induced acute lung injury [18], and the present study supported this. These findings suggest that the decrease in LPC may be associated with lipid metabolism in the lung during advanced fibrosis with ongoing inflammation.

Although a decrease in LPC has been reported, Rindlisbacher et al. observed that a structurally unidentified LPC was increased in PF [22]. In the present study, we found that LPC 20:5 was increased in PF, but could not confirm from the literature whether the unknown LPC is consistent with LPC20:5. An increase in LPC 18:0 has been reported in blood and lung tissue in a mouse bleomycin model of PF [19]. One of the possible reasons for the discrepancy among previous studies may be the use of different conditions or methods or the carrier protein of LPC [23]. Recent studies demonstrated that decreased levels of LPC were observed in various inflammatory and malignant diseases, where they were associated with increased mortality. In blood, LPC is mainly bound to albumin. Therefore, the pathophysiological condition can alter the ratio of free albumin bound to LPC, which affects the plasma levels of LPC [23].

Despite the discrepancy in reported LPC levels in PF, LPC 18:0 has been recognized as a sensitive marker for detecting PF and lung injury [18, 19]. Further studies are necessary to determine whether LPC 18:0 is useful for the early detection of active PF and the prediction of prognosis.

LPE was also decreased in PF patients compared with HC subjects. PE was metabolized to LPE by PLA2 [21], and the analysis of glycerophospholipid metabolic pathways in the present study also suggested that PLA2 was one of the enzymes involved in the conversion of PE to LPE. There were no previous reports of reduced LPE in patients with PF, but in chronic obstructive pulmonary disease (COPD), LPE was decreased in exacerbation and low pulmonary function. The role of LPE was speculated to be its anti-inflammatory effect [24], therefore reduced LPE may affect the progression of PF due to prolonged chronic inflammation. In contrast, LPE was elevated in the serum from a rat bleomycin-induced PF model, and elevated LPE was involved in deteriorating the vascular permeability and proliferation of fibroblasts [25]. It is conceivable that the level of LPE in PF may vary depending on the acute inflammatory phase or the chronic fibrosis phase.

In the present study, half of the extracted PE species were decreased, but the other half were increased in PF. For the mouse model of bleomycin-induced PF, PE treatment suppressed PF by suppressing collagen 1A1 production from fibroblasts and inducing the apoptosis of fibroblasts [26]. Although PE supplementation diminished PF [26], the present study showed that several PE were elevated in PF patients. Ferroptosis is an iron-dependent process of programmed cell death that is characterized by lipid peroxidation, and PE is an important signal of ferroptosis progression. Oxidized arachidonic and adrenic PE navigate cells to ferroptosis [27], and ferroptosis promotes PF through the fibroblast-to-myofibroblast transition [28]. Therefore, elevated PE may be correlated with the progression of ferroptosis in progressive PF. Overall, PE supplementation may not necessarily improve PF, but selective PE supplementation may be useful in the treatment of PF.

The importance of LPA signaling has been found in a wide variety of cells, including alveolar epithelial cells, vascular endothelial cells, and fibroblasts. Elevated LPA levels were reported in plasma, bronchoalveolar lavage fluid (BALF) and exhaled breath condensate (EBC) from PF patients [29–31]. While LPA was elevated in BALF, but plasma LPA was not different from that of normal subjects [31]. However, a decrease in plasma LPA in PF was observed in the present study. LPA is metabolized from LPC, and therefore, the reduced LPC in the present study may affect the reduced LPA. Another explanation for the discrepancy is that metabolites in EBC or BALF

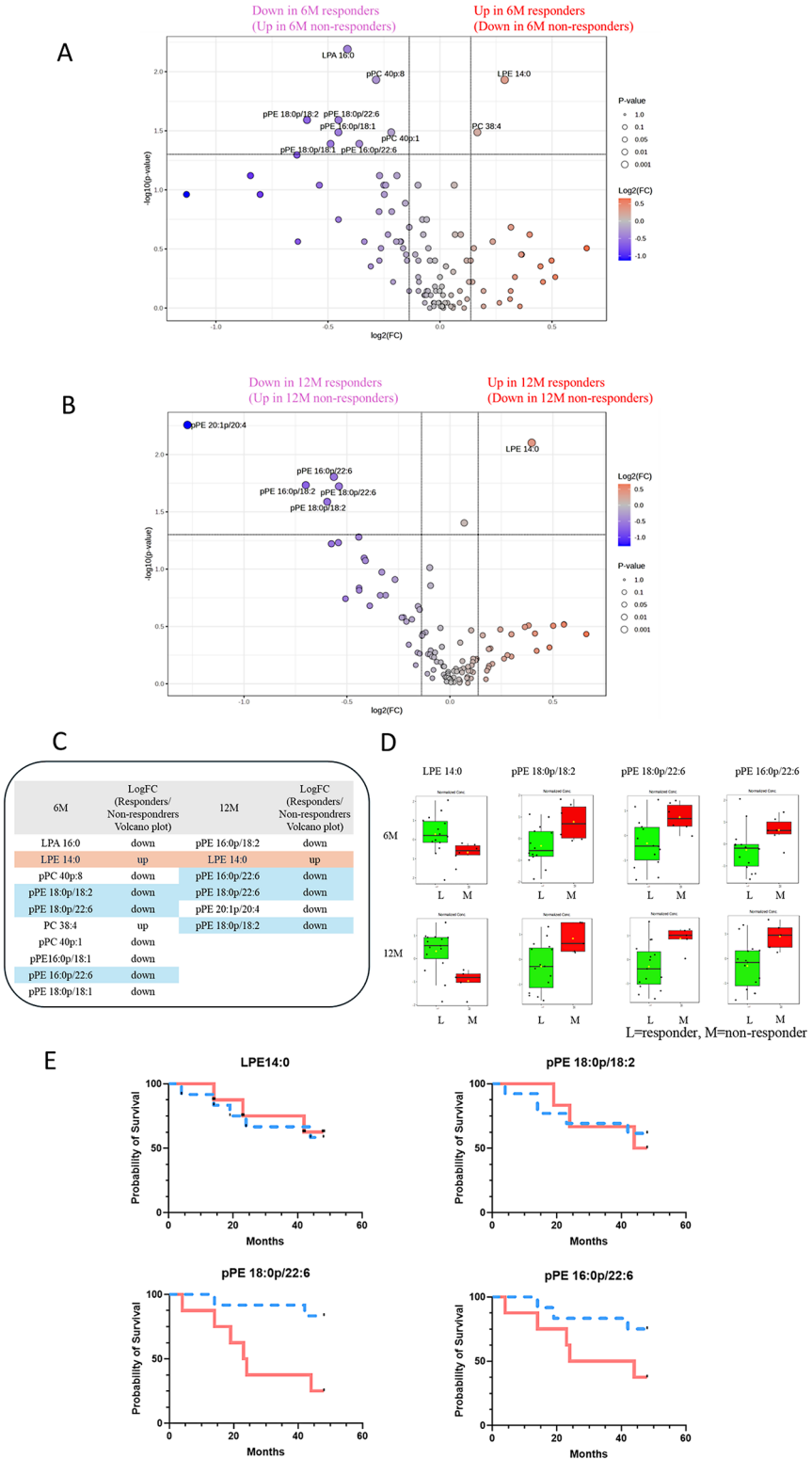

6M	LogFC (Responders/ Non-respondrers Volcano plot)	12M	LogFC (Responders/ Non-respondrers Volcano plot)
LPA 16:0	down	pPE 16:0p/18:2	down
LPE 14:0	up	LPE 14:0	up
pPC 40p:8	down	pPE 16:0p/22:6	down
pPE 18:0p/18:2	down	pPE 18:0p/22:6	down
pPE 18:0p/22:6	down	pPE 20:1p/20:4	down
PC 38:4	up	pPE 18:0p/18:2	down
pPC 40p:1	down		
pPE16:0p/18:1	down		
pPE 16:0p/22:6	down		
pPE 18:0p/18:1	down		

Fig. 5 (See legend on next page.)

(See figure on previous page.)

Fig. 5 (**A**) Volcano plot depicting the differential expression of lipids between those showing an absolute decline in %FVC < 2.5% (6 M responders) ($n = 14$) and a decline in %FVC > 2.5% (6 M non-responders) ($n = 6$) in PF patients at 6 M. (**B**) Volcano plot depicting the differential expression of lipids between those showing an absolute decline in %FVC < 5% (12 M responders) ($n = 15$) and a decline in %FVC > 5% (12 M non-responders) ($n = 5$). Lipids that were up-regulated with less decline in the %FVC are indicated in red, and those that were down-regulated with less decline in the %FVC are indicated in purple. (**C**) Lipids detected at both 6 M and 12 M. Red lipids were up-regulated and blue lipids were down-regulated in the 6 M responders and 12 M responders. (**D**) Distribution of lipids extracted at both 6 M and 12 M using box-and-whisker plots. (**E**) Lipids associated with 24 M survival after starting nintedanib. Lipid samples taken at 6 M were used for analysis. Patients were divided into two groups based on the median level of lipid from all samples at 6 M. The red line indicates patients with a lipid level above the median, and the blue line indicates patients with a lipid level below the median

and plasma do not always show similar fluctuation [31, 32]. The sampling site of the specimen may affect the observed levels of LPA. Different LPA and lipid species have been reported in IPF and other respiratory diseases. Variations in lipid extraction methods for measuring LPA species, whether or not a targeted assay was performed, and the lack of a common cutoff value for lipids may have resulted in different LPA levels between previous reports [29, 33, 34].

To summarize the findings regarding glycerophospholipid metabolism in Study 1, the reductions in LPC, LPA, and LPE were useful in discriminating PF patients from HC subjects. These decreased plasma lipids may be associated with progressive PF in an advanced inflammatory phase.

Sphingolipid metabolism and lipid levels were dysregulated in PF

Sphingolipid metabolism in PF showed decreased sphingolipids in the PF group compared with the HC group. Ceramide is one of the lipids that compose sphingolipids, and sphingomyelin (SM) is the pool molecule for the ceramide supply. Given that SM was decreased in PF patients, the decrease in ceramide may be a consequence of the decrease in SM. While there have been also reports showing a decrease of SM in PF [35], increased SM and ceramide have been reported in severe PF [36]. SM and ceramide levels may vary according to the severity of PF.

Considering each extracted sphingolipid, sphingosine-phosphate (S1P) d18:1 was decreased in PF patients in the present study. S1P regulates cell proliferation, inflammation, and vascular permeability [37]. In a murine model of LPS-induced lung injury, the administration of S1P within 6 h from the initiation of lung injury has been shown to dramatically reduce tissue damage and vascular leakage, suggesting that a substantial supply of S1P was effective for tissue repair [38]. Conversely, in vitro experiments have shown that S1P is elevated during the epithelial-to-mesenchymal transition, where excess S1P causes tissue damage [39], and S1P is elevated in PF patients [34]. From these findings, it is not clear whether altered S1P levels cause more injury or protection. S1P levels may show transient changes, and a decrease in S1P in PF may reflect acute vascular permeability due to vascular injury [38], whereas an increase in S1P may reflect the progression of fibrosis involving an epithelial-to-mesenchymal transition [39].

Ether lipid metabolism and lipid levels were dysregulated in PF

Ether lipid metabolism in PF showed that pPE and pPC levels differed between the PF and HC groups. pPEs, called plasmalogens, are a class of phospholipids carrying a vinyl ether bond at the sn-1 position and an ester bond at the sn-2 position of the glycerol backbone. pPCs have a similar structure to plasmalogens but contain a non-vinyl ether bond instead of the vinyl ether at the sn-1 position of the glycerol backbone [40–42]. pPE increases in response to elevated oxidative stress and reduces the stress by acting as a potential endogenous antioxidant [43, 44]. pPE is not only contained in surfactant obtained from alveolar type II cells but also involved in cellular components of polymorphonuclear cells and endothelial cells in the lung [45–47]. The biological roles of pPCs have remained unclear [41]; however, oxidized pPC contributed to maintaining the inflammatory state during atherosclerotic plaque formation [40]. Both pPE and pPC elevated transiently in response to hypoxia stress accompanied by a marked increase in the cell surface/volume ratio in endothelial cells in the hypoxia-induced pulmonary interstitial edema model in rabbits [48]. Synthesis of pPE and pPC are initiated at peroxisomes of intracellular organelles and transferred to the endoplasmic reticulum (ER) [41, 49]; therefore, dysregulation of the pathway in those organelles may be involved in PF development.

The pathway of ether lipids may be related to vascular lesions, and the pathway of glycerophospholipid May be related to fibrotic lesions in PF

The present study attempted to identify lipids related to endothelial cells and fibroblasts, as an ancillary experiment. In the comparison of the PF with HC groups in Study 1, increased pPE 38p:5 was a candidate for endothelial-related lipids, and an increased PE 32:1 and decreased PE 40:4 were candidates for fibroblast-related lipids. There are no previous reports describing the relationships between these lipids and PF. Comparing the PF and HC groups, considering that pPE was associated with

A

Lipids	Months in which differences could be detected between responders/non-responders	logFC for responders/non-responders	Endothelials-related	Fibroblasts-related
pPE 18:0p/22:6	6M, 12M	down	Up in endothelial cells	N/A
pPE 16:0p/22:6	6M, 12M	down	Up in endothelial cells	N/A
pPE 18:0p/18:2	6M, 12M	down	N/A	Up in myofibroblast transition
pPE 16:0p/18:1	6M	down	N/A	Up in myofibroblast transition
PC 38:4	6M	up	N/A	Down in myofibroblast transition

B

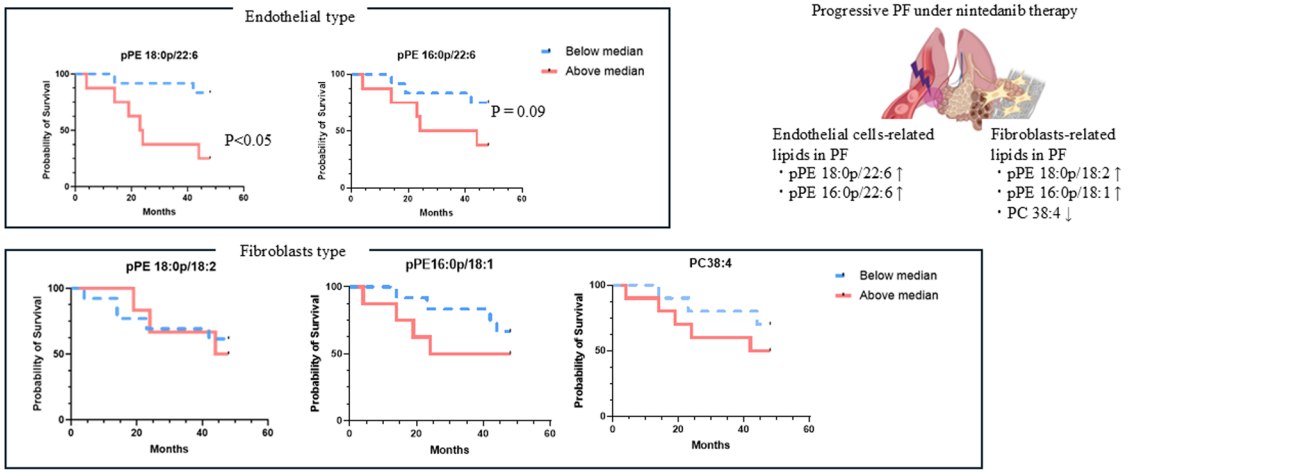

Fig. 6 Endothelial cell-related and fibroblast-related lipids and the patient survival for those lipids. (**A**) Two endothelial cell-related lipids and three fibroblast-related lipids were identified. (**B**) Lipids associated with 24 M survival after starting nintedanib. Patients were divided into two groups based on the median level of each lipid at 6 M. The red line indicates patients with a lipid level above the median, and the blue line indicates patients with a lipid level below the median

endothelial cells, the pathway of ether lipids appeared to correlate with vascular lesions. Additionally, PE was associated with fibroblasts, and thus the pathway of glycerophospholipid appeared to correlate with fibrotic lesions in PF.

Lipids discriminate the efficacy of nintedanib

In Study 2, the PF patients were divided into two groups based on the degree of decline in lung function at 6 M and 12 M after nintedanib administration, and the lipid levels were compared between the two groups. PC 38:4 was the top-scoring lipid for discrimination at 6 M, and PC 38:4 was down-regulated in the group with a greater decline in pulmonary function. Previous studies also demonstrated that PC 38:4 was decreased in PF [35], and PC38:4 was decreased during the fibroblast-to-myofibroblast transition [12]. PC 38:4 was also decreased with the inhibition of a major facilitator superfamily domain containing 2a (Mfsd2a), a sodium-dependent lysophosphatidylcholine (LPC) transporter of alveolar type II cells, and the transporter was important for the reuptake of LPC, which was produced from the hydrolysis of PC by secretory PLA2 [50]. Hence, the reduced level of PC 38:4 in plasma may indicate an altered phenotype of fibroblasts and/or impaired recycling system of surfactant in alveolar type II cells in more progressive PF.

Lipids associated with the survival of PF patients and the efficacy of nintedanib for suppressing the decline in %FVC

LPE 14:0 was the only elevated lipid in PF patients with less lung function decline. The anti-inflammatory effect of LPE was considered to be its major role [24]; therefore, reduced LPE may affect the progression of PF, and inversely, patients with higher LPE 14:0 are expected to exhibit less pulmonary function decline during nintedanib treatment.

Prognostic analysis was performed for 4 lipids, namely LPE14:0, pPE 16:0p/22:6, pPE 18:0p/22:6, and pPE 18:0p/18:2, extracted in Study 2. Among them, only pPE 18:0p/22:6 was associated with 24 M survival in plasma samples collected at 6 M. This result indicated that PF patients with high plasma pPE 18:0p/22:6 had a poorer prognosis despite the nintedanib treatment. In our previous study, the cellular component pPE 18:0p/22:6 was highest in mature vascular endothelial cells, with a significantly greater increase during differentiation from iPSC to vascular endothelial cells by the stimulation of VEGF, FGF2, and bone morphogenetic protein 4 (BMP4); in addition, pPE 18:0p/22:6 was higher in vascular endothelial cells than in fibroblasts [10]. Nintedanib is an inhibitor of VEGF-R, PDGF-R, and FGF-R. In this context, nintedanib cannot sufficiently suppress endothelial activation in patients showing high plasma pPE 18:0p/22:6, and PF patients with consistently high plasma

pPE 18:0p/22:6 may be characterized as the endothelial cell-damaged type, which may result in a poor response to nintedanib and poorer prognosis. It remains necessary to elucidate the precise molecular mechanisms by which abnormalities in endothelial cells lead to increased pPE.

Lipids related to endothelial cells and fibroblasts during nintedanib therapy and the survival of PF patients

All lipids detected in Study 2 were examined to determine whether they matched with endothelial cells or fibroblasts, referencing the previous experiment, as shown in supplemental TableS1. pPE 18:0p/22:6 and pPE 16:0p/22:6 were elevated and determined to be endothelial-related lipids. pPE 18:0p/22:6 is discussed in the previous section, but there have been no reports on pPE 16:0p/22:6 in lung diseases. The pPE 18:0p/22:6 levels were increased by tumor necrosis factor-α (TNF-α) in human umbilical vein endothelial cells (HUVEC) [25], and TNF-α, as well as TGF-β and endothelin-1, are key cytokines implicated in the pathogenesis of PF [51]. Therefore, the elevation of pPE 18:0p/22:6 may be associated with endothelial cell injury in PF; however, the precise roles of pPE 16:0p/22;6 in the lung have not been elucidated.

Among the lipids detected in Study 2, 2 lipids were matched to up-regulated lipids in the fibroblast-to-myofibroblast transition [12]. Elevated pPE 18:0p/18:2 and pPE 16:0p/18:1 were associated with decreased lung function despite nintedanibtreatment. To date, several studies regarding lipid metabolism in PF have reported on lipids that reflect the pulmonary surfactant and nutritional status associated with disease progression and treatment response for nintedanib [17, 22, 35]. pPE species are selectively synthesized from cytidine diphosphoethanolamine and diacylglycerol by ethanolamine phosphotransferase 1 (EPT1, also called selenoprotein I) in the ER of organelles during the synthesis of pPE. EPT1 plays an important role in the maintenance of pPE in skin fibroblasts and is expressed in the lungs [52]. Thus, the production of pPE 16:0p/18:2 and pPE 16:0p/18:1 may be increased by the activation of EPT1 in myofibroblasts involved in PF showing reduced lung function. Decreased PC 38:4 may relate not only to fibroblasts but also to the surfactant from alveolar type II cells, as discussed above.

In all endothelial cell-related lipids (i.e., pPE 16:0p/18:2 and pPE 18:0p/22:6) and fibroblast-related lipids (i.e., pPE 18:0p/18:2, pPE 16:0p/18:1, and PC 38:4), only pPE 18:0p/22:6 was significantly related to the 24 M survival in plasma samples collected at 6 M. Further studies are needed to determine how nintedanib affects pPE 18:0p/22:6 at the cellular level and clarify the clinical impact on PF, as well as determine whether pPE 18:0p/22:6 exhibits similar results during the treatment with other anti-fibrotic drugs such as pirfenidone and corticosteroids.

Limitations of this study

There were several limitations in the present study. First, the PF group was older and more often male than the HC group. This is mainly because it was difficult to obtain samples from elderly males without diseases. To minimize confounding factors between HC and PF would be desirable. Reasons why different lipid levels such as LPA, PC, and LPC among reports might arise from differences in the number and race of patients or HC, different lipid cutoff values in individual studies, and different extraction methods depending on the targeted lipids. Although there were no correlations between %FVC and the lipid levels, it would be meaningful to further deepen the test of correlation between other clinical parameters, e.g., diffusing capacity for carbon monoxide (DLCO) and lipids. Furthermore, there was no bias in the number of HC or PF patients, but the number of patients treated with nintedanib was small in Study 2 and survival was only followed up to 24 M. It is necessary to validate the results of this study by increasing the number of patients and extending the observation period. In addition, the lipid changes may not be specific to PF and should be investigated in other diseases. Although BALF was not analyzed in this study, it would be useful to simultaneously perform a highly sensitive lipid analysis on EBC to compare the local pulmonary pathology with plasma samples reflecting the overall metabolic abnormalities in patients with PF. It is also necessary to compare the changes in cellular metabolism during the transformations in other types of cells because epithelial cells and pericytes, not only fibroblasts, transform into myofibroblasts [3]. Moreover, nintedanib is an inhibitor of VEGF-R, PDGF-R, and FGF-R, and it is necessary to examine the lipid changes associated with the effect of nintedanib on vascular endothelial cell damage by generating an injured model using vascular endothelial cells and fibroblasts derived from PF patients. It may also be useful to compare the lipids detected in plasma with those detected in PF tissue samples by employing imaging-mass spectrometry [11, 53].

Conclusion

LPC and LPE were decreased in the plasma of PF patients, and the glycerophospholipid, sphingolipid, and ether lipid metabolism were altered in PF patients. pPE species were elevated in patients with reduced lung function despite nintedanib treatment; elevated pPE was assumed to be related to vascular endothelial cell components, and patients with pPE had poor prognosis. PF is a heterogeneous disease, but if we can provide a selective treatment according to the phenotype and provide precise medicine based on the unique lipid metabolism

associated with specific cell components, we can expand the scope of treatments. Examining lipid metabolism may also help in identifying phenotypes where drugs that had failed in previous clinical trials may be more effective. Samples from the lung regions appear to be desirable for validating lipid changes that relate to the progression of PF lesions, but sampling from the focal lung regions may not reflect the overall metabolism of the lung lesions or the patient's disease status. The clarification of various lipid species in the plasma may help to elucidate the pathophysiology of PF patients and support the development of new treatment options.

Supplementary Information

The online version contains supplementary material available at https://doi.org/10.1186/s12931-025-03239-0.

Supplementary Material 1

Supplementary Material 2

Supplementary Material 3

Supplementary Material 4

Supplementary Material 5

Supplementary Material 6

Supplementary Material 7

Supplementary Material 8

Supplementary Material 9

Supplementary Material 10

Acknowledgements
We thank Mio Fujimaki-Shiraishi (Dokkyo Medical University) for help with sample preparation and lipid extraction.

Author contributions
Conceptualization: Y.S. and H.S. Investigation Y.S., Y.N., T.Y., R.A., T. S., A.T., R.K., N.U., M.M., T.R., T.W., H.M., A.M., S.S., Y.H., and M.D. Statistical analysis and interpretation: K.I., Y.H., and M.D. Writing original draft preparation: Y.S. and Y.H. Writing-review and editing: S.N. Supervision Y.S., Y.H., M.D., and H.S. All authors contributed to the article and approved the submitted version.

Funding
A part of this research (Study 1) was supported by the Boehringer Ingelheim JP Science Research Promotion Fund 2023. The funder had no role in the interpretation of the data or design of the experiments.

Data availability
Trial registration: Lipidomic analysis on plasma in idiopathic pulmonary fibrosis patients. UMIN, UMIN000020872. Registered 3 February 2016, https://center6.umin.ac.jp/cgi-open-bin/ctr/index.cgi.The data set used and or analyzed during the current study is available from the corresponding author upon reasonable request with permission of the Dokkyo Medical University Hospital Ethical Committee. Owing to legal restrictions imposed by ethical committee-related personal information protection, the database cannot be made publicly available.

Declarations

Ethical approval and consent to participate
This study was conducted in accordance with the Declaration of Helsinki. All patients gave written informed consent before enrollment. This study was approved by The Human Research Committee of Dokkyo Medical University (number 27127).

Consent for publication
Not applicable.

Competing interests
The authors declare no competing interests.

Author details
[1]Department of Pulmonary Medicine and Clinical Immunology, Dokkyo Medical University, Mibu, Tochigi 321-0293, Japan
[2]Department of Biochemistry, Mibu, Tochigi 321-0293, Japan
[3]Kyushu Pro Search Limited Liability Partnership, 4-1, Kyudaishinmachi, Nishi-ku, Fukuoka 819-0388, Japan

Received: 5 December 2024 / Accepted: 16 April 2025
Published online: 28 April 2025

References

1. Raghu G, Collard HR, Egan JJ, Martinez FJ, Behr J, Brown KK, et al. An official ATS/ERS/JRS/ALAT statement: idiopathic pulmonary fibrosis: evidence-based guidelines for diagnosis and management. Am J Respir Crit Care Med. 2011;183:788–824.
2. Zhao X, Kwan JYY, Yip K, Liu PP, Liu FF. Targeting metabolic dysregulation for fibrosis therapy. Nat Rev Drug Discov. 2020;19:57–75.
3. Distler JHW, Györfi AH, Ramanujam M, Whitfield ML, Königshoff M, Lafyatis R. Shared and distinct mechanisms of fibrosis. Nat Rev Rheumatol. 2019;15:705–30.
4. May J, Mitchell JA, Jenkins RG. Beyond epithelial damage: vascular and endothelial contributions to idiopathic pulmonary fibrosis. J Clin Invest. 2023;133.
5. Krahn MP. Phospholipids of the plasma Membrane - Regulators or consequence of cell Polarity? Front Cell Dev Biol. 2020;8:277.
6. Shimizu Y. Phospholipid metabolism in stem cells and its application to the pathophysiological analysis. In: Haider KH, editor. Handbook of stem cell applications. Singapore: Springer Nature Singapore; 2023. pp. 1–16.
7. Fließer E, Jandl K, Lins T, Birnhuber A, Valzano F, Kolb D, et al. Lung fibrosis is linked to increased endothelial cell activation and dysfunctional vascular barrier integrity. Am J Respir Cell Mol Biol. 2024;71:318–31.
8. Zeinali S, Bichsel CA, Hobi N, Funke M, Marti TM, Schmid RA, et al. Human microvasculature-on-a Chip: anti-neovasculogenic effect of nintedanib in vitro. Angiogenesis. 2018;21:861–71.
9. Ackermann M, Werlein C, Plucinski E, Leypold S, Kühnel MP, Verleden SE et al. The role of vasculature and angiogenesis in respiratory diseases. Angiogenesis. 2024.
10. Nakamura Y, Shimizu Y, Horibata Y, Tei R, Koike R, Masawa M, et al. Changes of plasmalogen phospholipid levels during differentiation of induced pluripotent stem cells 409B2 to endothelial phenotype cells. Sci Rep. 2017;7:9377.
11. Shimizu Y, Nakamura Y, Horibata Y, Fujimaki M, Hayashi K, Uchida N, et al. Imaging of lysophosphatidylcholine in an induced pluripotent stem cell-derived endothelial cell network. Regen Ther. 2020;14:299–305.
12. Uchida N, Shimizu Y, Fujimaki M, Horibata Y, Nakamura Y, Horigane Y, et al. Metabolic changes induced by TGF-β1 via reduced expression of phosphatidylserine decarboxylase during myofibroblast transition. J Clin Biochem Nutr. 2022;70:108–16.
13. Nakamura Y, Shimizu Y. Cellular and molecular control of lipid metabolism in idiopathic pulmonary fibrosis: clinical application of the lysophosphatidic acid pathway. Cells. 2023;12.
14. Xia J, Wishart DS. Web-based inference of biological patterns, functions and pathways from metabolomic data using metaboanalyst. Nat Protoc. 2011;6:743–60.
15. Luo W, Brouwer C. Pathview: an R/Bioconductor package for pathway-based data integration and visualization. Bioinformatics. 2013;29:1830–1.
16. Luo W, Pant G, Bhavnasi YK, Blanchard SG Jr, Brouwer C. Pathview web: user friendly pathway visualization and data integration. Nucleic Acids Res. 2017;45(W1):W501–8.
17. Seeliger B, Carleo A, Wendel-Garcia PD, Fuge J, Montes-Warboys A, Schuchardt S, et al. Changes in serum metabolomics in idiopathic pulmonary fibrosis and effect of approved antifibrotic medication. Front Pharmacol. 2022;13:837680.

18. Saito K, Gemma A, Tatsumi K, Hattori N, Ushiki A, Tsushima K, et al. Identification and characterization of lysophosphatidylcholine 14:0 as a biomarker for drug-induced lung disease. Sci Rep. 2022;12:19819.
19. Lv W, Mao H, Ruan Y, Li S, Shimizu K, Zhang L, et al. Identification and immunological characterization of PLA2G2A and cell death-associated molecular clusters in idiopathic pulmonary fibrosis. Life Sci. 2023;331:122071.
20. Jaiswal A, Rehman R, Dutta J, Singh S, Ray A, Shridhar M et al. Cellular distribution of secreted phospholipase A2 in lungs of IPF patients and its Inhibition in Bleomycin-Induced pulmonary fibrosis in mice. Cells. 2023;12.
21. Tan ST, Ramesh T, Toh XR, Nguyen LN. Emerging roles of lysophospholipids in health and disease. Prog Lipid Res. 2020;80:101068.
22. Rindlisbacher B, Schmid C, Geiser T, Bovet C, Funke-Chambour M. Serum metabolic profiling identified a distinct metabolic signature in patients with idiopathic pulmonary fibrosis - a potential biomarker role for LysoPC. Respir Res. 2018;19:7.
23. Knuplez E, Marsche G. An updated review of Pro- and Anti-Inflammatory properties of plasma lysophosphatidylcholines in the vascular system. Int J Mol Sci. 2020;21.
24. Gai X, Guo C, Zhang L, Zhang L, Abulikemu M, Wang J, et al. Serum glycerophospholipid profile in acute exacerbation of chronic obstructive pulmonary disease. Front Physiol. 2021;12:646010.
25. Liu C, Lei S, Cai T, Cheng Y, Bai J, Fu W, et al. Inducible nitric oxide synthase activity mediates TNF-α-induced endothelial cell dysfunction. Am J Physiol Cell Physiol. 2023;325:C780–95.
26. Vazquez-de-Lara LG, Tlatelpa-Romero B, Romero Y, Fernández-Tamayo N, Vazquez-de-Lara F, J, MJ-J et al. Phosphatidylethanolamine induces an antifibrotic phenotype in normal human lung fibroblasts and ameliorates Bleomycin-Induced lung fibrosis in mice. Int J Mol Sci. 2018;19.
27. Kagan VE, Mao G, Qu F, Angeli JP, Doll S, Croix CS, et al. Oxidized arachidonic and adrenic PEs navigate cells to ferroptosis. Nat Chem Biol. 2017;13:81–90.
28. Lai W, Wang B, Huang R, Zhang C, Fu P, Ma L. Ferroptosis in organ fibrosis: from mechanisms to therapeutic medicines. J Transl Int Med. 2024;12:22–34.
29. Neighbors M, Li Q, Zhu SJ, Liu J, Wong WR, Jia G, et al. Bioactive lipid lysophosphatidic acid species are associated with disease progression in idiopathic pulmonary fibrosis. J Lipid Res. 2023;64:100375.
30. Tager AM, LaCamera P, Shea BS, Campanella GS, Selman M, Zhao Z, et al. The lysophosphatidic acid receptor LPA1 links pulmonary fibrosis to lung injury by mediating fibroblast recruitment and vascular leak. Nat Med. 2008;14:45–54.
31. Montesi SB, Mathai SK, Brenner LN, Gorshkova IA, Berdyshev EV, Tager AM, et al. Docosatetraenoyl LPA is elevated in exhaled breath condensate in idiopathic pulmonary fibrosis. BMC Pulm Med. 2014;14:5.
32. Cruickshank-Quinn C, Powell R, Jacobson S, Kechris K, Bowler RP, Petrache I, et al. Metabolomic similarities between Bronchoalveolar lavage fluid and plasma in humans and mice. Sci Rep. 2017;7:5108.
33. Suryadevara V, Ramchandran R, Kamp DW, Natarajan V. Lipid mediators regulate pulmonary fibrosis: potential mechanisms and signaling pathways. Int J Mol Sci. 2020;21.
34. Tanaka T, Koyama K, Takahashi N, Morito K, Ali H, Azuma M, et al. Lysophosphatidic acid, ceramide 1-phosphate and sphingosine 1-phosphate in peripheral blood of patients with idiopathic pulmonary fibrosis. J Med Invest. 2022;69:196–203.
35. Yan F, Wen Z, Wang R, Luo W, Du Y, Wang W, et al. Identification of the lipid biomarkers from plasma in idiopathic pulmonary fibrosis by lipidomics. BMC Pulm Med. 2017;17:174.
36. Summer R, Todd JL, Neely ML, Lobo LJ, Namen A, Newby LK, et al. Circulating metabolic profile in idiopathic pulmonary fibrosis: data from the IPF-PRO registry. Respir Res. 2024;25:58.
37. Jayant G, Kuperberg S, Somnay K, Wadgaonkar R. The role of sphingolipids in regulating vascular permeability in idiopathic pulmonary fibrosis. Biomedicines. 2023;11.
38. Wadgaonkar R, Patel V, Grinkina N, Romano C, Liu J, Zhao Y, et al. Differential regulation of sphingosine kinases 1 and 2 in lung injury. Am J Physiol Lung Cell Mol Physiol. 2009;296:L603–13.
39. Milara J, Navarro R, Juan G, Peiró T, Serrano A, Ramón M, et al. Sphingosine-1-phosphate is increased in patients with idiopathic pulmonary fibrosis and mediates epithelial to mesenchymal transition. Thorax. 2012;67:147–56.
40. Davies SS, Pontsler AV, Marathe GK, Harrison KA, Murphy RC, Hinshaw JC, et al. Oxidized alkyl phospholipids are specific, high affinity peroxisome proliferator-activated receptor gamma ligands and agonists. J Biol Chem. 2001;276:16015–23.
41. Dorninger F, Forss-Petter S, Wimmer I, Berger J. Plasmalogens, platelet-activating factor and beyond - Ether lipids in signaling and neurodegeneration. Neurobiol Dis. 2020;145:105061.
42. Koch J, Watschinger K, Werner ER, Keller MA. Tricky Isomers-The evolution of analytical strategies to characterize plasmalogens and plasmanyl ether lipids. Front Cell Dev Biol. 2022;10:864716.
43. Brosche T, Platt D. The biological significance of plasmalogens in defense against oxidative damage. Exp Gerontol. 1998;33:363–9.
44. Dean JM, Lodhi IJ. Structural and functional roles of ether lipids. Protein Cell. 2018;9:196–206.
45. Fehrenbach A, Ochs M, Warnecke T, Wahlers T, Wittwer T, Schmiedl A, et al. Beneficial effect of lung preservation is related to ultrastructural integrity of tubular Myelin after experimental ischemia and reperfusion. Am J Respir Crit Care Med. 2000;161:2058–65.
46. Seidl E, Kiermeier H, Liebisch G, Ballmann M, Hesse S, Paul-Buck K, et al. Lavage lipidomics signatures in children with cystic fibrosis and protracted bacterial bronchitis. J Cyst Fibros. 2019;18:790–5.
47. Zhuo R, Rong P, Wang J, Parvin R, Deng Y. The potential role of bioactive plasmalogens in lung surfactant. Front Cell Dev Biol. 2021;9:618102.
48. Botto L, Beretta E, Daffara R, Miserocchi G, Palestini P. Biochemical and morphological changes in endothelial cells in response to hypoxic interstitial edema. Respir Res. 2006;7:7.
49. Horibata Y, Ando H, Sugimoto H. Locations and contributions of the phosphotransferases EPT1 and CEPT1 to the biosynthesis of ethanolamine phospholipids. J Lipid Res. 2020;61:1221–31.
50. Wong BH, Mei D, Chua GL, Galam DL, Wenk MR, Torta F, et al. The lipid transporter Mfsd2a maintains pulmonary surfactant homeostasis. J Biol Chem. 2022;298:101709.
51. Coker RK, Laurent GJ. Pulmonary fibrosis: cytokines in the balance. Eur Respir J. 1998;11:1218–21.
52. Horibata Y, Elpeleg O, Eran A, Hirabayashi Y, Savitzki D, Tal G, et al. EPT1 (selenoprotein I) is critical for the neural development and maintenance of plasmalogen in humans. J Lipid Res. 2018;59:1015–26.
53. Nguyen SN, Kyle JE, Dautel SE, Sontag R, Luders T, Corley R, et al. Lipid coverage in nanospray desorption electrospray ionization mass spectrometry imaging of mouse lung tissues. Anal Chem. 2019;91:11629–35.

Publisher's note